UDC 621.3.013 https://doi.org/10.20998/2074-272X.2026.2.06

B.I. Kuznetsov, A.S. Kutsenko, T.B. Nikitina, I.V. Bovdui, K.V. Chunikhin, V.V. Kolomiets

The methodology of multi objective design of active-passive shielding system for overhead power lines magnetic field in residential buildings space based on metaheuristic optimization method

Problem. *Most studies of power frequency magnetic field reduced to safe level in in residential buildings located near overhead power lines carried out based on passive or active electromagnetic shielding, but there is no methodology for designing active-passive systems that include active and solid or multi-circuit passive shields. The* ***goal*** *of the work is to develop the methodology of multi objective design of active-passive electromagnetic shielding system, consisting of active and solid self or multi-circuit passive parts to improve shielding efficiency of initial magnetic field in residential building edges generated by overhead power lines to sanitary standards level. This goal proposed to achieve based on metaheuristic optimization method* ***Methodology.*** *Multi objective design methodology of active-passive shielding system based on solution of the geometric inverse problem of magnetostatics for the resulting magnetic field generated by the transmission line wires, compensation windings of the active shielding system and a passive shield in the form of a solid or multi-loop shield. The geometric forward problem is solved based on solutions of Maxwell's equation for magnetic field three-dimensional model using the COMSOL Multiphysics software. The solution of the geometric inverse problem of magnetostatics is formulated as a minimax vector problem of nonlinear programming. The solution of the minimax vector problem of nonlinear programming is calculated based on the metaeristic optimization algorithm from Pareto optimal solutions taking into account binary preference relations.* ***Results.*** *During combined active and solid or multi-circuit passive shielding system design spatial arrangement coordinates of solid or multi-loop passive shield and compensating windings, as well as windings currents and phases of active shield calculated. New scientific results are theoretical and experimental studies of a designed combined active and of solid or multi-circuit passive shielding system efficiency for magnetic field created by overhead power lines.* ***Scientific novelty****. For the first time multi objective design methodology for combined active and solid or multi-circuit passive shielding system taking into account original field shielding effectiveness decrease in residential building* edges *for more effective reduction of industrial frequency magnetic field created by overhead power lines developed.* ***Practical value****. Practical recommendations for the reasonable choice of the coordinates of the spatial arrangement of compensation windings of the active shielding system and a passive shield in the form of a solid or multi-loop shield, as well as the currents and phases in the compensation windings, parameters of regulators of the open and closed controls of the two degrees of freedom active shielding system and parameters of positions of magnetic field sensors of the active shielding system for magnetic field generated by overhead power lines in residential building space are given. The possibility of reducing the initial magnetic field induction to the sanitary standards level shown.* References 48, figures 11.

Key words: **overhead power line, magnetic field, combined electromagnetic active and passive shielding system, design computer simulation, experimental research.**

Проблема*. Більшість досліджень по зниженню рівня магнітного поля промислової частоти в житлових будинках, що розташовані поблизу повітряних ліній електропередачі, до безпечного рівня, виконані на основі пасивних або активних засобів електромагнітного екранування, але відсутня методологія проєктування активно-пасивних систем, які включають активні та суцільні або багатоконтурні пасивні екрани.* ***Метою*** *роботи є розробка методології багатоцільового проєктування активно-пасивної системи електромагнітного екранування, що складається з активних та суцільних або багатоконтурних пасивних частин для підвищення ефективності екранування вихідного магнітного поля на краях житлових будівель, що генерується повітряними лініями електропередачі, до рівня санітарних норм. Досягти зазначеної мети пропонується на основі методу метаевристичної оптимізації.* ***Методика****. Багатоцільове проєктування активно-пасивної системи екранування базується на розв'язанні геометричної оберненої задачі магнітостатики для результуючого магнітного поля, що генерується проводами лінії електропередачі, компенсаційними обмотками активної системи екранування та пасивним екраном у вигляді суцільного або багатоконтурного екрану. Геометрична пряма задача обчислюється на основі розв'язків рівняння Максвелла для тривимірної моделі магнітного поля за допомогою програмного забезпечення COMSOL Multiphysics. Розв'язок геометричної оберненої задачі магнітостатики формулюється як мінімаксна векторна задача нелінійного програмування. Розв'язок мінімаксної векторної задачі нелінійного програмування розраховується на основі метаевристичного алгоритму оптимізації, що базується на оптимальних за Парето розв'язках з урахуванням бінарних співвідношень переваги.* ***Результати****. В процесі багатоцільового проєктування активно-пасивної системи електромагнітного екранування розраховано координати просторового розташування суцільного або багатоконтурного пасивного екрану та компенсаційних обмоток системи активного екранування, а також струм та фази компенсуючих обмоток системи активного екранування. Новими науковими результатами є теоретичні та експериментальні дослідження ефективності синтезованої комбінованої активної та суцільної, або багатоконтурної, пасивної електромагнітних екрануючих систем магнітного поля, що створюється повітряними лініями електропередачі.* ***Наукова новизна.*** *Вперше розроблено методологію багатоцільового проєктування комбінованої активної та суцільної, або багатоконтурної, пасивної системи екранування з урахуванням ефективності екранування результуючого магнітного поля на краях житлових будівель для більш ефективного зменшення магнітного поля промислової частоти, що створюється повітряними лініями електропередачі.* ***Практична значимість****. Надано практичні рекомендації щодо обґрунтованого вибору координат просторового розташування компенсаційних обмоток системи активного екранування та пасивного екрану у вигляді суцільного, або багатоконтурного, екрану, а також струмів та фаз в компенсаційних обмотках, параметрів регуляторів розімкнутого та замкнутого управління системи активного екранування з двома ступенями свободи та параметрів положень датчиків магнітного поля системи активного екранування для магнітного поля, що генерується повітряними лініями електропередачі в просторі житлової забудови. Показана можливість зниження індукції вихідного магнітного поля до рівня санітарних норм*. Бібл. 48, рис. 11.

Ключові слова: **повітряна лінія електропередачі, магнітне поле, система комбінованого електромагнітного активного та пасивного екранування, проєктування, комп'ютерне моделювання, експериментальні дослідження.**

Introduction. Operating high-voltage overhead power lines, located in residential areas of most developed countries of the world, are the main sources of power frequency magnetic fields, which massively affect the population and are more dangerous to health than electric fields. At the end of the 20th century, experts from the World Health Organization discovered the carcinogenic properties of the power frequency magnetic field with its weak but long-term effect on humans [1]. Therefore, over the past 20 years, sanitary standards for the maximum permissible level of power frequency of 50-60 Hz for the population have been actively implemented and constantly

strengthened in the world, and intensive development of methods for normalizing power frequency magnetic fields is being carried out [2, 3].

Calculations and the results of numerous experiments show, the maximum permissible level of induction of power frequency magnetic fields at the border of sanitary protection zones of operating overhead lines, which were previously determined only by the EP, can be exceeded by more than an order of magnitude [3–5]. This poses a threat to the health of hundreds of thousands of people living closer than 100 m from the overhead line.

Fig. 1. Residential buildings located close to power line

As an example, Fig. 1 shows residential buildings located close to power line. From an economic point of view, methods of shielding residential buildings from magnetic field overhead lines are more promising [6, 7]. The economic significance of the work lies in normalizing the level of the magnetic field of industrial frequency in existing residential buildings located near overhead power lines, without decommissioning or reconstructing already operating overhead lines. The social significance of the work lies in ensuring the protection of public health from the negative effects of the man-made magnetic field of industrial frequency and, accordingly, extending the life expectancy of the population of Ukraine.

However, at present, the problem of effective shielding of power frequency magnetic fields of overhead lines has not been sufficiently studied. Methods of passive (electromagnetic) shielding of power frequency magnetic fields with conductive plates, which are traditional and effective for power frequency magnetic fields, when used for shielding magnetic fields of power frequency 50-60 Hz, require increased metal capacity, which within the framework of economic feasibility limits their efficiency to the level of 2-3, which in some cases is insufficient [8, 9]. In addition, traditional passive electromagnetic shield are airtight for air and opaque for light, which creates a problem of shielding window openings of residential buildings.

Active shielding methods of power frequency magnetic fields can be provided higher efficiency of shielding of overhead power lines (up to 10) with lower metal content [10–13]. Their essence lies in the automatic formation in a closed structure using special windings of compensating power frequency magnetic fields with such a space-time structure, the superposition of which with the power frequency magnetic fields of the overhead power line in the protection zone is minimized to a safe level [14–16]. The technology of active shielding of power frequency magnetic fields of operating overhead power lines has been used for more than 10 years by most developed countries of the world, for example, the USA, Italy, Spain and Israel [17, 18].

However, methods and means of increasing the characteristics of both active and passive shielding systems of residential buildings for effective protection of their residents from the effects of overhead power lines remain undeveloped [19–26]. Also, the methods of active and passive shielding do not have a theoretical and experimental justification, and the criteria for their rational use depending on the design and localization of overhead power lines relative to the residential building have not been determined [26–28]. The idea of the research is to optimize the systems of active and passive shielding of overhead power lines in residential buildings depending on the spatial structure of the overhead power lines, which is determined by the design and localization of overhead power lines, as well as the use of transparent lattice electromagnetic shielding for residential buildings.

When designing combined electromagnetic shield, it is necessary to reduce the level of the initial magnetic field in the entire shielding space along the length, width and height of the residential building [29–31]. Therefore, it is necessary to use a three-dimensional model of the magnetic field. Moreover, the need to use passive shielding may be needed precisely at the edges of the residential building [32–34]. When designing combined electromagnetic shielding, it is necessary to take into account the inaccurate knowledge of the parameters of the initial magnetic field, as well as their change during operation, and therefore the designed system must be robust [35–37].

Therefore, the problem of designing combined electromagnetic shielding taking into account the uncertainties of the initial magnetic field model is reduced to solving a minimax vector optimization problem with constraints [38–40]. The components of the vector objective function are the values of the induction of the resulting magnetic field at the considered points of the shielding space. These components of the vector objective function are nonlinear nonconvex functions and contain a set of local extrema [41–43].

To solve such complex, multidimensional nonlinear and nonconvex optimization problems, metaheuristic group intelligence algorithms are widely used [31, 32].

The **goal** of the work is to develop the methodology of multi objective design of active-passive electromagnetic shielding system, consisting from active and solid or multi-circuit passive parts to improve shielding efficiency of initial magnetic field in residential building edges generated by overhead power lines to sanitary standards level. This goal proposed to achieve based on metaheuristic optimization method.

Definition of geometric forward magnetostatic problem for passive solid electromagnetic shield. The most widespread method of reducing the magnetic field level is electromagnetic shielding using a solid passive shield. The geometric forward problem of magnetostatics for solid passive electromagnetic shield is to calculate the secondary three-dimensional model of magnetic field generated by a solid passive electromagnetic shield placed in the original magnetic field. It is assumed that the coordinates of the spatial location, geometric dimensions and electrical parameters – electrical and magnetic conductivity of the solid passive electromagnetic shield are specified. Naturally, the original magnetic field is also considered specified.

To model electromagnetic processes in a solid passive electromagnetic shield, the COMSOL Multiphysics software is used to solve Maxwell's equations using the finite element method for three-dimensional models of the electromagnetic field in the following form.

Gauss's law for electric field

$$\nabla \cdot \boldsymbol{E} = \frac{\rho}{\varepsilon_0}; \quad (1)$$

Gauss's law for magnetism

$$\nabla \cdot \boldsymbol{B} = 0; \quad (2)$$

Faraday's law for electromagnetic induction

$$\nabla \times \boldsymbol{E} = -\frac{\partial \boldsymbol{B}}{\partial t}; \quad (3)$$

Ampere's loop law

$$\nabla \times \boldsymbol{B} = \mu_0 \boldsymbol{J} + \mu_0 \varepsilon_0 \frac{\partial \boldsymbol{E}}{\partial t}, \quad (4)$$

where vector $\boldsymbol{E}$ is electric field strength; vector $\boldsymbol{B}$ is magnetic flux density; vector $\boldsymbol{J}$ is current density; ρ is electric charge density.

To study the process of electromagnetic shielding of a three-phase power line through which a harmonic current flows in a steady state, the law of the total current in integral form, written in a quasi-stationary approximation in terms of complex amplitudes, was used:

$$\oint_l \boldsymbol{H}\,\mathrm{d}l = \int_S \gamma \boldsymbol{E}\,\mathrm{d}S + \int_S \boldsymbol{J}^{ext}\,\mathrm{d}S, \quad (5)$$

where $\boldsymbol{H}$, $\boldsymbol{E}$ – complex amplitudes of the intensity vectors of the magnetic and electric fields, respectively; $\boldsymbol{J}^{ext}$ – complex amplitude of the current density vector of external sources; γ – specific electrical conductivity; l – contour covering the integration surface S.

Equation (1) can be written in the form:

$$\oint_l \frac{1}{\mu} \mathrm{rot}\,\boldsymbol{A}^*\,\mathrm{d}l = -j\mu_0\omega \cdot \int_S \gamma \boldsymbol{A}^*\,\mathrm{d}S + \mu_0 \cdot \int_S \boldsymbol{J}^{ext}\,\mathrm{d}S, \quad (6)$$

where $\boldsymbol{A}^*$ is the vector magnetic potential; μ is the relative magnetic permeability; $\mu_0 = 4\pi \cdot 10^{-7}$ H/m is the magnetic constant; ω is the circular frequency.

The obtained equation describes the distribution of vector magnetic potential in the system «solid electromagnetic shield – current sources of magnetic field». The electromagnetic shield is given by its geometric parameters, relative magnetic permeability μ and specific electrical conductivity γ. For the external environment, we can set μ=1, γ=0. The system of current sources is described by the frequency ω and the current density distribution vector $\boldsymbol{J}^{ext}$. In this case, the current conductors are considered as current filaments.

Numerical modeling of electromagnetic processes in systems with extended current conductors and thin-walled open-circuited conductive shielding elements is based on the combined use of finite difference methods and absorbing boundary conditions, the division of the computational domain into a number of additional subdomains containing thin-walled elements, and the use of a non-uniform computational grid to calculate the field in the thickness of the shield walls with subsequent «stitching» of the solutions obtained in each subdomain [44, 45].

The computational domain contains current conductors, an electromagnetic shield and a protected area. Uniaxial well-matched layers are introduced at the boundaries of the computational domain: this additional medium occupies several cells of the computational grid and plays an auxiliary role, and its anisotropic parameters ensure fast and non-reflective attenuation of the electromagnetic field in it. Therefore, at its outer boundary, the value of the vector magnetic potential can be set equal to zero: $\boldsymbol{A}^* = 0$. The computational domain was divided into a number of additional subdomains, some of which contained thin-walled conductive elements. A rectangular grid was imposed in each subdomain, and the step inside the shielding elements was smaller. The solutions obtained in each subdomain were «stitched» at their boundaries [46].

Let us define the vector $\boldsymbol{X}_{pss}$ of the sought parameters of solid passive electromagnetic shield, the components of which are coordinates of the spatial location, geometric dimensions and electrical parameters – electrical and magnetic conductivity of the solid passive electromagnetic shield. Such three-dimensional numerical modeling allows us to calculate instantaneous value of a vector $\boldsymbol{B}_{pss}(\boldsymbol{X}_{pss}, P_i, t)$ of induction of the three-dimensional model of magnetic field generated by solid electromagnetic shield at the point P_i of the shielding space at the moment of time t. Therefore, the geometric forward problem of magnetostatics for a solid passive electromagnetic shield is solved.

Definition of geometric forward magnetostatic problem for multi-circuit passive electromagnetic shield. The geometric forward problem of magnetostatics for multi-circuit passive electromagnetic shield is to calculate the secondary three-dimensional model of magnetic field generated by a multi-circuit passive electromagnetic shield placed in the original magnetic field [26]. It is assumed that the coordinates of the spatial location, geometric dimensions and electrical parameters – electrical and magnetic conductivity of multi-circuit passive electromagnetic shield are specified. Naturally, the original magnetic field is also considered specified.

Multi-circuit passive shield consist of a set of aluminum wires that are interconnected in a certain way and form current circuit. In most cases, all the wires of the shield are connected in parallel. The wires are arranged parallel to each other and parallel to the overhead line, which provides the greatest shielding efficiency. The calculation of the magnetic field of multi-circuit passive shield can be carried out by analytical, semi-analytical or numerical methods.

For given initial magnetic field induction vector $\boldsymbol{B}_{Ra}(Q_i, \boldsymbol{X}_a, \boldsymbol{\delta}, t)$ as well as of geometric dimensions vector values $\boldsymbol{X}_p$ of multi-circuit passive contour shield, magnetic flux $\boldsymbol{\Phi}_l(\boldsymbol{X}_a, \boldsymbol{X}_p, \boldsymbol{\delta}, t)$ piercing contour l of multi-circuit passive shield calculated [26]

$$\boldsymbol{\Phi}_l\left(\boldsymbol{X}_a, \boldsymbol{X}_p, \boldsymbol{\delta}, t\right) = \int_S \boldsymbol{B}_{Ra}(\boldsymbol{X}_a, \boldsymbol{\delta}, t)\,\mathrm{d}S. \quad (7)$$

Current $\boldsymbol{I}_{Pl}(\boldsymbol{X}_a, \boldsymbol{X}_p, \boldsymbol{\delta}, t)$ in complex form, induced in circuit l of multi-circuit passive shield calculated according to Ohm law and in integral form of Faraday law [19]:

$$\boldsymbol{I}_{Pl}\left(\boldsymbol{X}_a, \boldsymbol{X}_p, \boldsymbol{\delta}, t\right) = -j\omega\boldsymbol{\Phi}(\boldsymbol{X}_a, \boldsymbol{X}_p, \boldsymbol{\delta}, t)/\ldots \\ \ldots/(\boldsymbol{R}_l(\boldsymbol{X}_p) + j\omega\boldsymbol{L}_l(\boldsymbol{X}_p)), \quad (8)$$

where $\boldsymbol{R}_l(\boldsymbol{X}_p)$ – active resistance and inductance $\boldsymbol{L}_l(\boldsymbol{X}_p)$ of circuit l of multi-circuit passive shield calculated for passive shield geometric dimensions vector values $\boldsymbol{X}_p$.

In the numerical method of calculating the three-dimensional model of the magnetic field of multi-circuit

passive shield, the coordinates of the spatial arrangement of the wires, the geometric dimensions of these wires and the electrical conductivity of the shield wires are given. The entire calculation area is divided into sub-areas, each of which is aluminum or air. During the calculation, discrete calculation mesh were superimposed, the types and sizes of which differed significantly according to the calculation sub-area. The presented model allows you to calculate the electric currents induced in the screen and, accordingly, find the three-dimensional model of of the shielded magnetic field distribution.

Let us define the vector $\boldsymbol{X}_{pcs}$ of the sought parameters of multi-circuit passive electromagnetic shield, the components of which are coordinates of the spatial location, geometric dimensions and electrical parameters – electrical and magnetic conductivity of multi-circuit passive electromagnetic shield. Such three-dimensional numerical modeling allows us to calculate instantaneous value of a vector $\boldsymbol{B}_{pcs}(\boldsymbol{X}_{pcs}, P_i, t)$ of induction of the three-dimensional model of magnetic field generated by multi-circuit electromagnetic shield at the point P_i of the shielding space at the moment of time t. Therefore, the geometric forward problem of magnetostatics for a multi-circuit passive electromagnetic shield is solved.

Definition of geometric forward magnetostatic problem for active quasi-static electromagnetic shield. Let's first consider a quasi-static formulation of the forward magnetostatic problem of current regulation in the compensation windings of an active shielding system. This direct problem involves calculating a three-dimensional model of the magnetic field generated by the compensation windings of an active shielding system. It is assumed that the spatial coordinates of these compensation windings of the active shielding system are specified, as are the instantaneous current values – the amplitudes and phases of the currents in these compensation windings of the active shielding system.

Three-dimensional model is calculated the magnetic field inside a residential building and represents the compensation windings of the active shielding system as a set of current conductors, while the influence of other elements is not taken into account. The general method of calculating the three-dimensional model of magnetic field based on the Biot-Savart law. The essence of the method is that the conductors are replaced by a broken line consisting of straight segments. A current $i(t)$ flows through each infinitely thin segment of the conductor with a dl length. According to the Biot-Savart law, the current $i(t)$ flowing through the segment dl generates a magnetic field with induction:

$$\mathrm{d}\boldsymbol{B}(t) = \frac{\mu_0 \mathrm{i}(t)}{4\pi R^3}(\mathrm{d}\boldsymbol{l} \times \boldsymbol{R}). \qquad (9)$$

Then we can calculate the magnetic field induction generated by the entire compensation winding.

$$\boldsymbol{B}(t) = \frac{\mu_0 \mathrm{i}(t)}{4\pi} \int_{-L}^{L} \frac{(\mathrm{d}\boldsymbol{l} \times \boldsymbol{R})}{R^3}, \qquad (10)$$

where it is assumed that the integration is carried out along a line segment $(-L,+L)$ along which the unit vector is directed.

Let us define the vector $\boldsymbol{X}_{aqs}$ of the sought geometric parameters of compensation windings of an active shielding system, the components of which are coordinates of the spatial location, geometric dimensions compensation windings of an active shielding system.

Let us define also the vector $\boldsymbol{I}_{aqs}$ of sought electric parameters of compensation windings of an active shielding system, the components of which are current in these compensation windings of an active shielding system.

Such three-dimensional numerical modeling allows us to calculate based on the Biot-Savart law (6) instantaneous value of a vector $\boldsymbol{B}_{aqs}(\boldsymbol{X}_{aqs}, \boldsymbol{I}_{aqs}, P_i, t)$ of induction of the three-dimensional model of magnetic field generated by active quasi-static electromagnetic shield at the point P_i of the shielding space at the moment of time t. Therefore, the geometric forward problem of magnetostatics for active quasi-static electromagnetic shield is solved.

Definition of geometric forward magnetostatic problem for magnetic field sensors positions of active electromagnetic shield. The active shielding system is a multi-channel dynamic automatic control system, the number of channels in which is determined by the number of compensation windings. This active shielding system is a two-degree-of-freedom system and simultaneously includes open and closed control loops. The forward objective of designing an active shielding system is to calculate the currents in the compensation windings of the active shielding system using magnetic field sensors. Moreover, to implement closed-loop control, the magnetic field sensors are installed within the shielding space.

The number of these magnetic field sensors is usually equal to the number of compensation windings in the active shielding system. To implement open-loop current control in the compensation windings of the active shielding system, the magnetic field sensor is installed outside the shielding space. Typically, to implement open current control loops in all compensation windings of the active shielding system, one magnetic field sensor is used, which is installed at a significant distance from the shielding space. In this case, it is assumed that the voltages at the outputs of the magnetic field sensors, which are used to implement open and closed loops for regulating currents in the compensation windings of the active shielding system, are specified.

The geometric forward magnetostatic problem for positions of magnetic field sensors of active electromagnetic shield is to calculate the output of the magnetic field sensors, which is necessary for implementing open and closed loop current control in the compensation windings of the active shielding system. In this case, it is naturally assumed that the spatial coordinates and spatial orientation angles of these magnetic field sensors are specified. Naturally, the magnetic field at the location of these magnetic field sensors is also assumed to be known.

Let's first consider definition of geometric forward magnetostatic problem for magnetic field sensors positions of active electromagnetic shield. We introduce the induction vector $\boldsymbol{B}_R(t)$ the components of which are induction vectors $\boldsymbol{B}_R(Q_i,t)$ of the resulting magnetic field at points Q_i of magnetic field sensors installed. We also introduce the unit vectors $\boldsymbol{\varphi}$ of the angular positions of the

magnetic field sensors and column vector $\boldsymbol{K}_M$ of the gain coefficients of the magnetic field sensor taking into account the number of turns of their measuring coils and the gains of the preamplifiers.

Then the vector $\boldsymbol{y}_s(t)$ of sensor output voltage will take the following form

$$\boldsymbol{y}_S(t) = \boldsymbol{B}_R(t) \otimes \varphi \otimes \boldsymbol{K}_M + \boldsymbol{w}(t), \qquad (11)$$

where the sign $\otimes$ denotes the tensor (Kronecker) product of the column vectors; $\boldsymbol{w}(t)$ is the magnetometer noise vector.

The components of the sensor output voltage vector $\boldsymbol{y}_s(t)$ are instantaneous values of projections of the components of the induction vectors $\boldsymbol{B}_R(Q_i, t)$ of the resulting magnetic field in sensors installed points Q_i on the components of unit vectors $\boldsymbol{\varphi}$ of the angular position of the magnetic field sensors taking into account the components of column vector $\boldsymbol{K}_M$ of the magnetic field sensor gain coefficients.

Let's define a vector $\boldsymbol{X}_{asp}$ of positions of magnetic field sensors for active dynamic electromagnetic shield, whose components are the vector of spatial coordinates Q_i and the vector of angular positions $\boldsymbol{\varphi}$ of the magnetic field sensor. Then, for a given vector $\boldsymbol{X}_{asp}$, based on (7), a geometric forward magnetostatic problem for magnetic field sensors positions of active electromagnetic shield can be solved – the vector of instantaneous values of the magnetic field sensor output voltages can be calculated.

Definition of forward problem for active dynamic electromagnetic shield. Let us now consider the forward problem for active dynamic electromagnetic shield of calculating the currents $\boldsymbol{I}_w(t)$ in the compensation windings of the active shielding system using a dynamic system with two degrees of freedom based on the output voltages $\boldsymbol{y}_s(t)$ of the magnetic field sensors.

Let us introduce the vector $\boldsymbol{X}_{ars}$, the components of which are the parameters of the open and closed controllers $\boldsymbol{R}(\boldsymbol{X}_{ars})$, with the help of which control with two degrees of freedom is implemented. Then, based on the vectors $\boldsymbol{y}_s(t)$ of instantaneous values of the output voltages of the magnetic field sensors using the regulators of the open and closed controls of the two degrees of freedom active shielding system, a vector $\boldsymbol{I}_w(t)$ of instantaneous values of the currents in the cleanliness windings can be calculated.

$$\boldsymbol{I}_w(t+1) = \boldsymbol{R}(\boldsymbol{X}_{ars})\boldsymbol{y}_S(t). \qquad (12)$$

Definition of geometric inverse magnetostatic problem for combined electromagnetic shield. The resulting magnetic field in the shielding space is a superposition of the original magnetic field generated by the transmission line wires and the combined electromagnetic shield. The combined electromagnetic shield includes the active shield windings and a passive solid or multi-circuit shield.

In most works devoted to the calculation of the electromagnetic field of power transmission lines, the sagging of the wires on the field distribution is not taken into account. The wires are assumed to be infinite, rectilinear and parallel to the earth's surface. The advantage of this approach is that it allows the problem of calculating the magnetic field to be considered in a two-dimensional setting. However, research results have shown that neglecting the effect of sagging when calculating the magnetic field can lead to an error of 45 %.

Therefore, when calculating the magnetic field of overhead power lines, we will take into account the sagging of the wires. It is assumed that the wires have the shape of a catenary line, and in this case the problem of calculating the magnetic field is three-dimensional.

Let us define the vector $\boldsymbol{X}_{ipl}$ of the parameters of overhead power lines, the components of which are are coordinates of the spatial location and geometric dimensions of overhead power lines wires as wel as vector $\boldsymbol{X}_{ipl}$ of amplitudes A_i and phases φ_i of currents in power transmission lines wires.

Currents in transmission lines exhibit daily, weekly, seasonal, and annual variations. Let's define the uncertainty vector $\boldsymbol{\delta}$ of the initial magnetic field generated by the transmission line. Then, the vector $\boldsymbol{B}_{ipl}(\boldsymbol{\delta}, P_i, t)$ of the instantaneous value at time t of the resulting magnetic space point P_i can be calculated as a three-dimensional model based on the Biot-Savart law (10).

Such three-dimensional numerical modeling allows us to calculate the distributions of the induction of the three-dimensional model of magnetic field generated by the transmission line wires, that is, to solve the geometric forward problem of magnetostatics for transmission line wires.

Let us first consider the problem of compensating for the initial magnetic field generated by the power transmission line wires using a combined shield in a quasi-static setting. For given vectors of parameters of a solid passive electromagnetic shield $\boldsymbol{X}_{pss}$, a multi-circuit passive electromagnetic shield $\boldsymbol{X}_{pcs}$ and geometric $\boldsymbol{X}_{aqs}$ and currents $\boldsymbol{I}_{aqs}$ parameters of compensation windings of an active shielding system in a quasi-stationary setting based on the solution of geometric forward problems, the instantaneous values of the magnetic field induction vectors $\boldsymbol{B}_{pss}(\boldsymbol{X}_{pss}, P_i, t)$ generated by solid passive electromagnetic shield vectors $\boldsymbol{B}_{pcs}(\boldsymbol{X}_{pcs}, P_i, t)$ generated by multi-circuit passive electromagnetic shield vectors $\boldsymbol{B}_{aqs}(\boldsymbol{X}_{aqs}, \boldsymbol{I}_{aqs}, P_i, t)$ generated by compensation windings of an active shielding system at the moment of time t in space point P_i can be calculated.

Let us introduce the vector $\boldsymbol{X}$ of the required parameters of the design of a combined shield, the components of which are vectors of parameters of a solid passive electromagnetic shield $\boldsymbol{X}_{pss}$, a multi-circuit passive electromagnetic shield $\boldsymbol{X}_{pcs}$ and geometric $\boldsymbol{X}_{aqs}$ and currents $\boldsymbol{I}_{aqs}$ parameters of compensation windings of an active shielding system in a quasi-stationary setting

$$\boldsymbol{X} = \left(\boldsymbol{X}_{pss}, \boldsymbol{X}_{pcs}, \boldsymbol{X}_{aqs}, \boldsymbol{I}_{aqs}\right). \qquad (13)$$

Then the instantaneous value of the vector $\boldsymbol{B}_R(\boldsymbol{X}, \boldsymbol{\delta}, P_i, t)$ of the resulting magnetic field induction is calculated as the following sum

$$\begin{aligned}\boldsymbol{B}_R(\boldsymbol{X}, \boldsymbol{\delta}, P_i, t) = \boldsymbol{B}_{ipl}(\boldsymbol{\delta}, P_i, t) + \boldsymbol{B}_{pss}\left(\boldsymbol{X}_{pss}, P_i, t\right) + \\ + \boldsymbol{B}_{pcs}\left(\boldsymbol{X}_{pcs}, P_i, t\right) + \boldsymbol{B}_{aqs}\left(\boldsymbol{X}_{aqs}, \boldsymbol{I}_{aqs}, P_i, t\right)\end{aligned} \qquad (14)$$

Let us now consider the problem of compensation of the initial magnetic field generated by the power transmission line wires using a combined shield in a dynamic setting taking into account the solution to the problem of spatial placement and angular position of magnetic field sensors, as well as the design of active

shielding system controllers as a dynamic system with two degrees of freedom. In contrast to the quasi-static formulation of the problem of designing a combined shield, when the currents in the compensation windings of the active shielding system are the desired parameters, in the dynamic formulation of the problem of designing a combined shield, when the currents in the compensation windings of the active shielding system are calculated using a dynamic system with two degrees of freedom.

For the given values of the vector $\boldsymbol{X}_{asp}$ of the sought parameters of the spatial and angular positions of the magnetic field sensors, the output voltages $\boldsymbol{y}_s(t)$ of the magnetic field sensors are calculated based on the solution of the geometric forward problem. Naturally, when calculating the output voltages of the magnetic field sensors, the calculated values of the vector $\boldsymbol{B}_R(Q_i, t)$ of resulting magnetic field at the installation points Q_i of the magnetic field sensors inside the shielding space are used to implement closed-loop control algorithms for the currents of the compensation windings of the active shielding system.

When calculating the output voltage $\boldsymbol{y}_s(t)$ of the initial magnetic field sensors, the calculated values of the initial magnetic field $\boldsymbol{B}_{ipl}(Q_i, t)$ at the installation points Q_i of the magnetic field sensor outside the shielding space are used to implement open-loop control algorithms for the currents of the compensation windings of the active shielding system. For the given values of the vector $\boldsymbol{X}_{ars}$ of the parameters of the active shielding system regulators, the vector $\boldsymbol{I}_w(t)$ of instantaneous values of the currents in the compensation windings of the active shielding system are calculated based on the calculated output voltages $\boldsymbol{y}_s(t)$ of the magnetic field sensors. Then, for the values of currents $\boldsymbol{I}_w(t)$ in the compensation windings of the active dynamic shielding system calculated in this way and for the given values of the vector $\boldsymbol{X}_{aqs}$ of the sought geometric parameters of compensation windings of an active shielding system, the value of instantaneous value of induction vector $\boldsymbol{B}_{ads}(\boldsymbol{X}_{aqs}, \boldsymbol{X}_{asp}, \boldsymbol{X}_{ars}, P_i, t)$ is calculated.

Then three-dimensional numerical modeling allows us to calculate based on the Biot-Savart law (10) instantaneous value of a vector $\boldsymbol{B}_{ads}(\boldsymbol{X}_{aqs}, \boldsymbol{X}_{asp}, \boldsymbol{X}_{ars}, P_i, t)$ of induction of the three-dimensional model of magnetic field generated by active dynamic electromagnetic shielding system at the point P_i of the shielding space at the moment of time t. Therefore, the geometric forward problem of magnetostatics for active dynamic electromagnetic shielding system is solved.

Let us introduce the vector $\boldsymbol{X}$ of the required parameters of the design of combined shield with dynamic electromagnetic shielding system, the components of which are vectors of parameters of a solid passive electromagnetic shield $\boldsymbol{X}_{pss}$, a multi-circuit passive electromagnetic shield $\boldsymbol{X}_{pcs}$, geometric parameters $\boldsymbol{X}_{aqs}$ of compensation windings of an active shielding system, positions $\boldsymbol{X}_{asp}$ of magnetic field sensors for active dynamic electromagnetic shield and regulator parameters $\boldsymbol{X}_{ars}$ of active dynamic electromagnetic shielding system

$$\boldsymbol{X} = \left(\boldsymbol{X}_{pss}, \boldsymbol{X}_{pcs}, \boldsymbol{X}_{aqs}, \boldsymbol{X}_{asp}, \boldsymbol{X}_{ars}\right). \qquad (15)$$

Then the instantaneous value of the vector $\boldsymbol{B}_R(\boldsymbol{X}, \boldsymbol{\delta}, P_i, t)$ of the resulting magnetic field induction is calculated as the following sum

$$\begin{aligned}\boldsymbol{B}_R\left(\boldsymbol{X}, \boldsymbol{\delta}, P_i, t\right) = \boldsymbol{B}_{ipl}\left(\boldsymbol{\delta}, P_i, t\right) + \boldsymbol{B}_{pss}\left(\boldsymbol{X}_{pss}, P_i, t\right) + \\ \boldsymbol{B}_{pcs}\left(\boldsymbol{X}_{pcs}, P_i, t\right) + \boldsymbol{B}_{aqs}\left(\boldsymbol{X}_{aqs}, \boldsymbol{X}_{asp}, \boldsymbol{X}_{ars}, P_i, t\right)\end{aligned} \qquad (16)$$

The requirements for the resulting magnetic field level apply not to the instantaneous value $\boldsymbol{B}_R(\boldsymbol{X}, \boldsymbol{\delta}, P_i, t)$ of the magnetic field induction vector, but to its effective value. Therefore, based on the instantaneous value $\boldsymbol{B}_R(\boldsymbol{X}, \boldsymbol{\delta}, P_i, t)$ of magnetic field induction vector we calculated effective value $\boldsymbol{B}_R(\boldsymbol{X}, \boldsymbol{\delta}, P_i)$ of resulting magnetic field induction in shielding space point P_i. A safe magnetic field level for habitation is usually regulated throughout the entire shielding space, so we introduce a vector $\boldsymbol{B}_R(\boldsymbol{X}, \boldsymbol{\delta})$ of effective magnetic field values. Its components are the effective magnetic field values $\boldsymbol{B}_R(\boldsymbol{X}, \boldsymbol{\delta}, P_i)$ at individual points P_i of the shielding space, covering the entire shielding space

$$\boldsymbol{B}_R\left(\boldsymbol{X}, \boldsymbol{\delta}\right) = \left(\boldsymbol{B}_R\left(\boldsymbol{X}, \boldsymbol{\delta}, P_1\right), \boldsymbol{B}_R\left(\boldsymbol{X}, \boldsymbol{\delta}, P_2\right), \ldots \boldsymbol{B}_R\left(\boldsymbol{X}, \boldsymbol{\delta}, P_n\right)\right)^T. \qquad (17)$$

Then the problem of designing a combined shield is reduced to solving a nonlinear minimax vector optimization problem $\boldsymbol{B}_R(\boldsymbol{X}, \boldsymbol{\delta})$. In the process of this problem solving it is necessary to minimize $\boldsymbol{B}_R(\boldsymbol{X}, \boldsymbol{\delta})$) (14) or (16) by the vector $\boldsymbol{X}$ (9) or (15) of sought parameters, but to maximize this same $\boldsymbol{B}_R(\boldsymbol{X}, \boldsymbol{\delta})$ by the vector $\boldsymbol{\delta}$ of uncertainty parameters.

Metaheuristic optimization algorithm. A distinctive feature of the nonlinear minimax vector optimization problem (15) or (17) is its multi-extremality, which is due to the nature of the original nonlinear functions. Furthermore, the scalar objective functions that are components of the vector objective function are antagonistic. This is due to the nature of the compensation of the initial magnetic field at a specific point in the shielding space. When minimizing the magnetic field level at a particular point in the shielding space, the magnetic field level at other points in the shielding space increases due to undercompensation or overcompensation of the original magnetic field using a combined electromagnetic shield.

To solve such complex, nonlinear and multidimensional optimization problems metaheuristic algorithms of group intelligence are widely used. From metaheuristic algorithms the most widely used are genetic optimization, particle swarm optimization (PSO), white whale optimization, gray wolf optimization, wind driven optimization, bacterial foraging optimization algorithm, binary particle swarm optimization, harmony search algorithm, flower pollination algorithm, harmony flower pollination algorithm, multiverse optimization algorithm, coco search algorithm and many other algorithms that model the group intelligence of the behavior of a swarm of living organisms. To improve computing capabilities, a combination of these metaheuristic algorithms is used, and these evolutionary algorithms of group intelligence are also used simultaneously with deterministic algorithms – sequential quadratic programming, Levenberg-Marquardt algorithms and many others.

Currently, it seems that various types of heuristic algorithms based on PSO are most widely used.

Consider calculated nonlinear minimax vector optimization problem based on PSO. Let's first look initial value of sought parameters vector $\boldsymbol{X}$ and external parametric perturbations vectors $\boldsymbol{\delta}$. for nonlinear minimax vector optimization problem calculated by PSO.

Nonlinear minimax vector optimization problem required parameters (17) desired parameters vectors $\boldsymbol{X}$ and uncertainties parameters vectors $\boldsymbol{\delta}$. It is necessary to minimize nonlinear minimax vector optimization problem (17) by parameters vectors $\boldsymbol{X}$ but maximize the same nonlinear minimax vector optimization problem by uncertainty parameters vector $\boldsymbol{\delta}$. Therefore, each particle i of swarm j included both position $x_{ij}(t)$, $\delta_{ij}(t)$ and velocity $v_{ij}(t)$, $u_{ij}(t)$ components for both required vector $\boldsymbol{X}$ and vector $\boldsymbol{\delta}$ calculated.

$$x_{ij}(t+1) = x_{ij}(t) + v_{ij}(t+1); \tag{18}$$

$$\delta_{ij}(t+1) = \delta_{ij}(t) + u_{ij}(t+1), \tag{19}$$

where

$$v_{ij}(t+1) = w_j v_{ij}(t) + c_{1j} r_{1j}(t) H\left(p_{1j} - \varepsilon_{1j}(t)\right)\left[y_{ij}(t) - \ldots \right. \\ \left. \ldots - {}_{ij}(t)\right] + c_{2j} r_{2j}(t) H\left(p_{2j} - \varepsilon_{2j}(t)\right)\left[y^*_j(t) - x_{ij}(t)\right]; \tag{20}$$

$$u_{ij}(t+1) = w_j u_{ij}(t) + c_{1j} r_{1j}(t) H\left(p_{1j} - \varepsilon_{1j}(t)\right)\left[z_{ij}(t) - \ldots \right. \\ \left. \ldots - \delta_{ij}(t)\right] + c_{2j} r_{2j}(t) H\left(p_{2j} - \varepsilon_{2j}(t)\right)\left[z^*_j(t) - \delta_{ij}(t)\right] \tag{21}$$

In fact, all varieties of PSO algorithms are implementations of random search algorithms of first-order order. In this case, the role of the derivative is played by the random direction in which the change in the objective function is greatest. It is well known that first-order methods are most effective when searching far from the optimum. As the optimum is approached, the rate of change of the objective function decreases, and consequently, the effectiveness of first-order methods declines. Furthermore, as the extremum is approached, zigzag movements are possible, with the extremum point jumping. In a nearly stationary region, second-order methods are more effective, using both first and second derivatives to find the extremum.

Let us consider a heuristic algorithm for random search based on a swarm of particle motion, which simultaneously uses the velocities and accelerations of particles – analogs of the first and second derivatives, calculated on the basis of random search [47]. Let us denote the initial values of the vectors $\boldsymbol{X}_{ij}(t)$ and $\boldsymbol{\delta}_{ij}(t)$, which are calculated using the PSO. Then the step $\boldsymbol{d}_{ijx}(t)$ of further changing the vector $\boldsymbol{X}_{ij}(t)$ is calculated as the solution of the problem of minimizing the quadratic objective function.

Minimize

$$\left\langle \boldsymbol{F}(\boldsymbol{X}_{ij}(t), \boldsymbol{\delta}_{ij}(t)) \right\rangle + 1/2 \boldsymbol{d}^T_{ijx}(t) \boldsymbol{H}_{ijx}(t) \boldsymbol{d}_{ijx}(t) + \ldots \\ \ldots + J^T_{ijx}(t) \boldsymbol{d}_{ijx}(t). \tag{22}$$

Also the step $\boldsymbol{d}_{ij\delta}(t)$ of further changing the vector $\boldsymbol{\delta}_{ij}(t)$ is calculated as the solution of the problem of maximizing the quadratic objective function.

Maximize

$$\left\langle \boldsymbol{F}(\boldsymbol{X}_{ij}(t), \boldsymbol{\delta}_{ij}(t)) \right\rangle + 1/2 \boldsymbol{d}^T_{ij\delta}(t) \boldsymbol{H}_{ij\delta}(t) \boldsymbol{d}_{ij\delta}(t) + \ldots \\ \ldots + J_{ij\delta}{}^T(t) \boldsymbol{d}_{ij\delta}(t). \tag{23}$$

In these both quadratic objective function (22), (23) the components of Jacobian matrices $\boldsymbol{J}_{ijx}(t)$, $\boldsymbol{J}_{ij\delta}(t)$ and Hessian matrices $\boldsymbol{H}_{ijx}(t)$, $\boldsymbol{H}_{ij\delta}(t)$, respectively, along vectors $\boldsymbol{X}_{ij}(t)$ and $\boldsymbol{\delta}_{ij}(t)$ calculated from velocities $v_{ij}(t)$, $u_{ij}(t)$ and accelerations $A_{ijx}(t)$, $A_{ij\delta}(t)$ of particle i of swarm j movement from $x_{ij}(t)$, $\delta_{ij}(t)$ positions.

Particles movement accelerations $A_{ijx}(t)$, $A_{ij\delta}(t)$ calculated based on velocities $v_{ij}(t)$, $u_{ij}(t)$ as

$$A_{ijx}(t+1) = v_{ij}(t+1) - v_{ij}(t); \tag{24}$$

$$A_{ij\delta}(t+1) = u_{ij}(t+1) - u_{ij}(t). \tag{25}$$

Then, to minimize nonlinear minimax vector optimization problem by $\boldsymbol{X}_{ij}(t)$ and to maximize nonlinear minimax vector optimization problem by $\delta_{ij}(t)$ step size optimal values $d_{ijx}(t)$ and $d_{ij\delta}(t)$ calculated as

$$A_{ijx}(t) d_{ijx}(t) + v_{ij}(t) = 0; \tag{26}$$

$$A_{ij\delta}(t) d_{ij\delta}(t) + u_{ij}(t) = 0. \tag{27}$$

And then particle motion calculated as

$$x_{ij}(t+1) = x_{ij}(t) + \alpha_{ijx}(t) d_{ijx}(t); \tag{28}$$

$$\delta_{ij}(t+1) = \delta_{ij}(t) + \alpha_{ij\delta}(t) d_{ij\delta}(t). \tag{29}$$

In conclusion, we note that to calculate the optimal values of the motion steps $\boldsymbol{d}_{ijx}(t)$ and $\boldsymbol{d}_{ij\delta}(t)$ to minimize the objective function (22) and maximize the objective function (23), it is necessary to calculate the inverse Hessian matrices $\boldsymbol{H}_{ijx}(t)$, $\boldsymbol{H}_{ij\delta}(t)$, respectively, along vectors $\boldsymbol{X}_{ij}(t)$ and $\boldsymbol{\delta}_{ij}(t)$. Random search of this matrices are calculated from velocities $v_{ij}(t)$, $u_{ij}(t)$ and accelerations $A_{ijx}(t)$, $A_{ij\delta}(t)$ of particle i of swarm j movement from $x_{ij}(t)$, $\delta_{ij}(t)$ positions. To improve computational efficiency, a stochastic analogue of the Levenberg-Marquardt algorithm is used. The step sizes are calculated as

$$\left\{ \boldsymbol{J}_{ijx}{}^T(t) \boldsymbol{J}_{ijx}(t) + \lambda_t diag\left[\boldsymbol{J}_{ijx}{}^T(t) \boldsymbol{J}_{ijx}(t) \right] \right\} \boldsymbol{d}_{ijx}(t) = \\ = -\boldsymbol{J}_{ijx}{}^T(t) \boldsymbol{F}(\boldsymbol{X}_{ij}(t), \boldsymbol{\delta}_{ij}(t); \tag{30}$$

$$\left\{ \boldsymbol{J}_{ij\delta}{}^T(t) \boldsymbol{J}_{ij\delta}(t) + \lambda_t diag\left[\boldsymbol{J}_{ij\delta}{}^T(t) \boldsymbol{J}_{ij\delta}(t) \right] \right\} \boldsymbol{d}_{ij\delta}(t) = \\ = -\boldsymbol{J}_{ij\delta}{}^T(t) \boldsymbol{F}(\boldsymbol{X}_{ij}(t), \boldsymbol{\delta}_{ij}(t). \tag{31}$$

In this case, there is no need to calculate the inverse Hessian matrix and particle motion calculated by (28, 29).

When nonlinear minimax vector optimization problem global optimum calculated from Pareto sets of optimal solutions it is necessary binary preference relations used [31, 32].

Simulation results. As an example, Fig. 2 shows three-dimensional magnetic field level distribution with combined shield with of a multi-circuit passive shield when only one passive shield is operating (*a*), when only one active shield is operating (*b*), and when a combined shield with a multi-circuit passive shield is operating (*c*). As can be seen from Fig. 2,*a*, when only one multi-loop passive shield is in operation, the level of induction in the shielding space is practically independent of the width of the passive shield. As can be seen from Fig. 2,*b*, when only one active shield is in operation, the level of induction in the shielding space is approximately 2–3 times lower than when only one multi-circuit passive shield is in operation. Moreover, the level of induction in the shielding space increases significantly at the edges of the shielding zone, which is due to the finite length of the compensation windings of the active shield. As can be seen from Fig. 2,*c*, when operating a combined shield with a multi-contour passive shield, the level of induction in the shielding space is practically independent of the width of the passive shield.

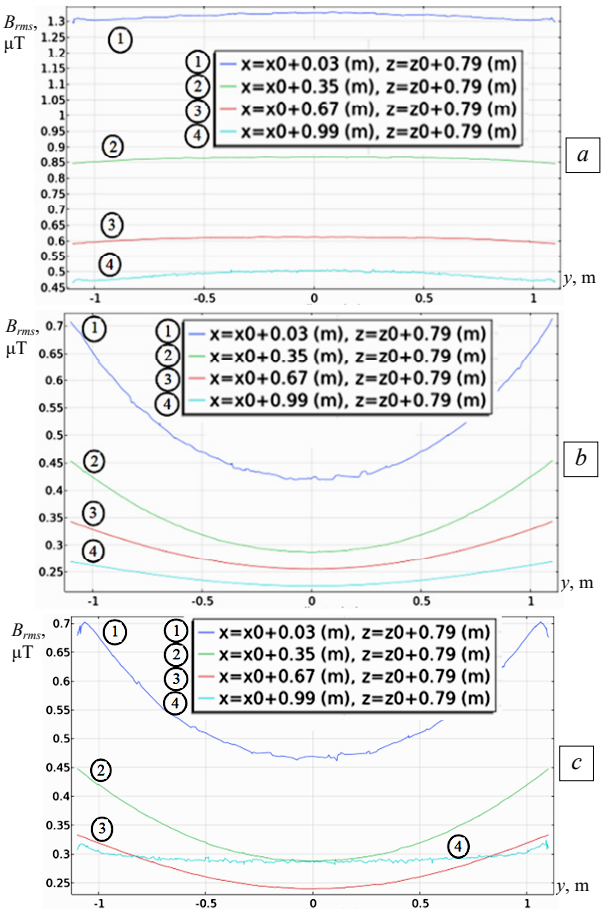

Fig. 2. Three-dimensional magnetic field level distribution with combined shield with multi-circuit passive shield

As a second example, Fig. 3 shows three-dimensional magnetic field level distribution with combined shield with solid passive shield when operating a combined shield with continuous passive shield without (*a*) and with side plates (*b*).

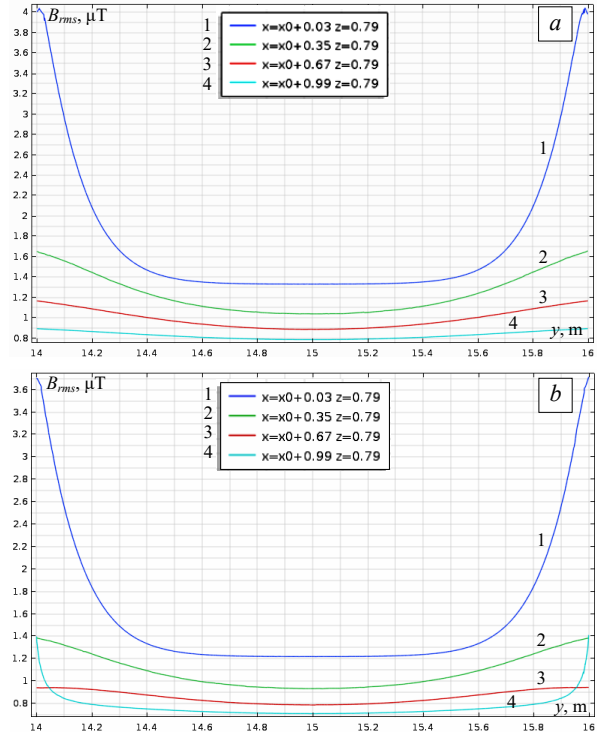

Fig. 3. Three-dimensional magnetic field level distribution with combined shield with solid passive shield

As follows from the comparison of these distributions of magnetic field induction, when using side plates from a continuous passive shield, the level of induction at the edges of the shielding space decreases compared to a continuous passive shield without side plates.

Experimental setup of a combined electromagnetic shielding systems. To conduct comprehensive experimental studies, an experimental setup of a combined electromagnetic shield was developed [48].

Figure 4 shows a solid passive shield without side plates. Figure 5 shows a solid passive shield with side plates on either side of the shield.

Figure 6 shows a multi-circuit passive shield.

Fig. 4. Solid passive shield without side plates

Fig. 5. Solid passive shield with side plates on either side of the shield

Fig. 6. Multi-circuit passive shield

Figure 7 shows the active shield compensation windings. This figure also shows magnetometers installed in the shielding space and designed to provide feedback on the resulting magnetic field. Figure 8 shows the power amplifiers for powering the active shield compensation windings. Figure 9 shows the electronic part of the control system for the active shield compensation windings.

Fig. 7. Active shield compensation windings

Fig. 8. Power amplifiers for powering the active shield compensation windings

Fig. 9. Control system electronic part for active shield compensation windings

Experimental studies results. Figure 10 shows experimentally measured three-dimensional magnetic field level distribution with combined shield with of a multi-circuit passive shield when only one passive shield is operating (*a*), when only one active shield is operating (*b*), and when a combined shield with a multi-circuit passive shield is operating (*c*). As can be seen from Fig. 10,*a*, when only one multi-loop passive shield is in operation, the level of induction in the shielding space is practically independent of the width of the passive shield. As can be seen from Fig. 10,*b*, when only one active shield is in operation, the level of induction in the shielding space is approximately 2–3 times lower than when only one multi-circuit passive shield is in operation. Moreover, the level of induction in the shielding space increases significantly at the edges of the shielding zone, which is due to the finite length of the compensation windings of the active shield. As can be seen from Fig. 10,*c*, when operating a combined shield with a multi-contour passive shield, the level of induction in the shielding space is practically independent of the width of the passive shield.

Figure 11 shows experimentally measured three dimensions magnetic field level distribution with combined shield with solid passive shield during operation of a combined shield with a continuous passive shield without (*a*) and with side plates (*b*).

How should these experimental distributed magnetic field inductions be compared, using side plates of a continuous passive screen, induction in the central part and at the edges of the screen, displacement of space compared to continuous passive light without side plates.

Based on the comparison of the experimentally measured three dimensions magnetic field level distribution (Fig. 10, 11) and the results of modeling three-dimensional magnetic field level distribution (Fig. 2, 3), we can conclude that experimentally measured induction levels values of magnetic field distribution coincide with calculated magnetic field distributions with 20 % accuracy.

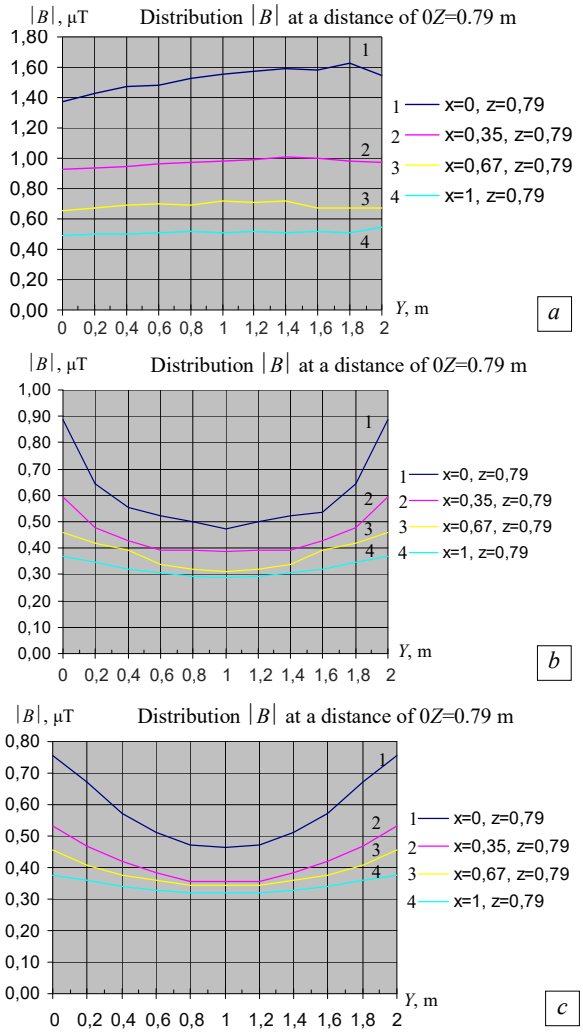

Fig. 10. Experimentally measured three dimensions magnetic field level distribution with combined shield with multi-circuit passive shield

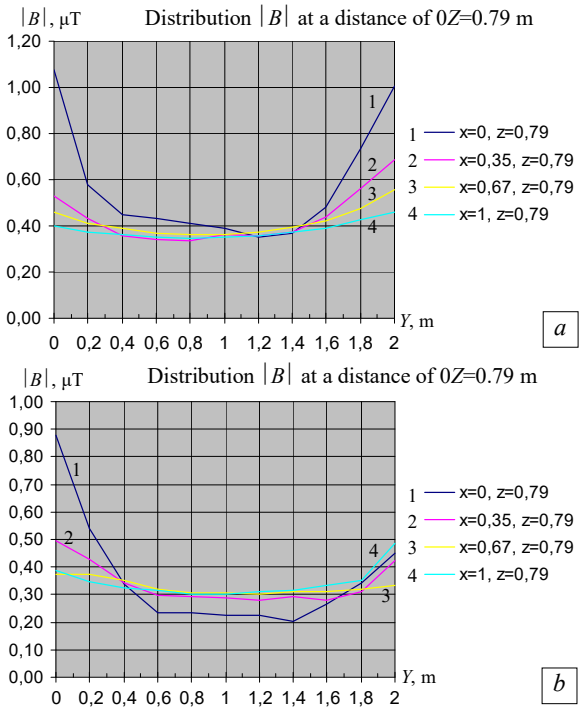

Fig. 11. Experimentally measured three dimensions magnetic field level distribution with combined shield with solid passive shield

Conclusions.

1. For the first time methodology of multi objective design of active-passive electromagnetic shielding system, consisting of active and solid self or multi-circuit passive parts, based on metaheuristic optimization algorithm developed, which allows to improve shielding efficiency of initial magnetic field in residential building edges generated by overhead power lines to sanitary standards level.

2. A new solution method for active-passive shielding system design developed based on solution of the geometric inverse problem of magnetostatics for the resulting magnetic field generated by the transmission line wires, which made it possible to calculate the coordinates of the spatial arrangement of compensation windings of the active shielding system and a passive shield in the form of a solid or multi-loop shield, as well as the currents and phases in the compensation windings, parameters of regulators of the open and closed controls of the two degrees of freedom active shielding system and parameters of positions of magnetic field sensors of the active shielding system.

3. A new solution method for geometric inverse problem based on minimax vector nonlinear programming problem is proposed. The geometric forward problem solved based on Maxwell's equation solutions for magnetic field three-dimensional model using the COMSOL Multiphysics software. The minimax vector nonlinear programming problem calculated based on the metaeristic optimization algorithm point from Pareto optimal solutions taking into account binary preference relations, which allows to reduce the computation time.

4. Results of theoretical and experimental studies of different types designed combined active and solid or multi-circuit passive shielding system efficiency for magnetic field created by overhead power lines are given. Results of experimental studies confirmed the correctness of the main theoretical principles. Experimentally measured induction levels values of resulting magnetic field distribution coincide with calculated magnetic field distributions with 20 % accuracy.

5. Practical recommendations for the reasonable choice of the coordinates of the spatial arrangement of compensation windings of the active shielding system and a passive shield in the form of a solid or multi-loop shield, as well as the currents and phases in the compensation windings, parameters of regulators of the open and closed controls of the two degrees of freedom active shielding system and parameters of positions of magnetic field sensors of the active shielding system for magnetic field generated by overhead power lines in residential building space are given.

6. It is planned to practically realization of developed methodology for the multi objective design of active-passive electromagnetic shielding systems of magnetic fields for residential buildings located near 110 kV overhead power transmission lines to normalize magnetic field level in real residential building.

Conflict of interest. The authors declare that they have no conflicts of interest.

REFERENCES

1. Sung H., Ferlay J., Siegel R.L., Laversanne M., Soerjomataram I., Jemal A., Bray F. Global Cancer Statistics 2020: GLOBOCAN Estimates of Incidence and Mortality Worldwide for 36 Cancers in 185 Countries. *CA: A Cancer Journal for Clinicians*, 2021, vol. 71, no. 3, pp. 209-249. doi: https://doi.org/10.3322/caac.21660.

2. *Directive 2013/35/EU of the European Parliament and of the Council of 26 June 2013 on the minimum health and safety requirements regarding the exposure of workers to the risks arising from physical agents (electromagnetic fields)*. Available at: http://data.europa.eu/eli/dir/2013/35/oj (Accessed 20 May 2025).

3. *The International EMF Project. Radiation & Environmental Health Protection of the Human Environment World Health Organization*. 1996. 2 p. Available at: https://www.who.int/initiatives/the-international-emf-project (Accessed 20 May 2025).

4. Rozov V.Y., Reutskiy S.Y., Pelevin D.Y., Kundius K.D. Magnetic field of electrical heating cable systems of the floors for residential premises. *Electrical Engineering & Electromechanics*, 2024, no. 5, pp. 48-57. doi: https://doi.org/10.20998/2074-272X.2024.5.07.

5. Rozov V.Y., Reutskiy S.Y., Kundius K.D. Protection of workers against the magnetic field of 330-750 kV overhead power lines when performing work without removing the voltage under load. *Electrical Engineering & Electromechanics*, 2024, no. 4, pp. 70-78. doi: https://doi.org/10.20998/2074-272X.2024.4.09.

6. Rozov V.Y., Pelevin D.Y., Kundius K.D. Simulation of the magnetic field in residential buildings with built-in substations based on a two-phase multi-dipole model of a three-phase current conductor. *Electrical Engineering & Electromechanics*, 2023, no. 5, pp. 87-93. doi: https://doi.org/10.20998/2074-272X.2023.5.13.

7. Rozov V.Y., Pelevin D.Y., Reutskiy S.Y., Kundius K.D., Vorushylo A.O. The complex influence of external and internal electricity networks on the magnetic field level in residential premises of buildings. *Electrical Engineering & Electromechanics*, 2025, no. 4, pp. 11-19. doi: https://doi.org/10.20998/2074-272X.2025.4.02.

8. Salceanu A., Paulet M., Alistar B.D., Asiminicesei O. Upon the contribution of image currents on the magnetic fields generated by overhead power lines. *2019 International Conference on Electromechanical and Energy Systems (SIELMEN)*. 2019. doi: https://doi.org/10.1109/sielmen.2019.8905880.

9. Del Pino Lopez J.C., Romero P.C. Influence of different types of magnetic shields on the thermal behavior and ampacity of underground power cables. *IEEE Transactions on Power Delivery*, Oct. 2011, vol. 26, no. 4, pp. 2659-2667. doi: https://doi.org/10.1109/tpwrd.2011.2158593.

10. Hasan G.T., Mutlaq A.H., Ali K.J. The Influence of the Mixed Electric Line Poles on the Distribution of Magnetic Field. *Indonesian Journal of Electrical Engineering and Informatics (IJEEI)*, 2022, vol. 10, no. 2, pp. 292-301. doi: https://doi.org/10.52549/ijeei.v10i2.3572.

11. Victoria Mary S., Pugazhendhi Sugumaran C. Investigation on magneto-thermal-structural coupled field effect of nano coated 230 kV busbar. *Physica Scripta*, 2020, vol. 95, no. 4, art. no. 045703. doi: https://doi.org/10.1088/1402-4896/ab6524.

12. Ippolito L., Siano P. Using multi-objective optimal power flow for reducing magnetic fields from power lines. *Electric Power Systems Research*, 2004, vol. 68, no. 2, pp. 93-101. doi: https://doi.org/10.1016/S0378-7796(03)00151-2.

13. Barsali S., Giglioli R., Poli D. Active shielding of overhead line magnetic field: Design and applications. *Electric Power Systems Research*, May 2014, vol. 110, pp. 55-63. doi: https://doi.org/10.1016/j.epsr.2014.01.005.

14. Bavastro D., Canova A., Freschi F., Giaccone L., Manca M. Magnetic field mitigation at power frequency: design principles and case studies. *IEEE Transactions on Industry Applications*, May 2015, vol. 51, no. 3, pp. 2009-2016. doi: https://doi.org/10.1109/tia.2014.2369813.

15. Beltran H., Fuster V., García M. Magnetic field reduction screening system for a magnetic field source used in industrial applications. *9 Congreso Hispano Luso de Ingeniería Eléctrica (9 CHLIE)*, 2005, pp. 84-99.

16. Bravo-Rodríguez J., Del-Pino-López J., Cruz-Romero P. A Survey on Optimization Techniques Applied to Magnetic Field Mitigation in Power Systems. *Energies*, 2019, vol. 12, no. 7, art. no. 1332. doi: https://doi.org/10.3390/en12071332.

17. Canova A., del-Pino-López J.C., Giaccone L., Manca M. Active Shielding System for ELF Magnetic Fields. *IEEE Transactions on Magnetics*, March 2015, vol. 51, no. 3, pp. 1-4. doi: https://doi.org/10.1109/tmag.2014.2354515.

18. Canova A., Giaccone L. Real-time optimization of active loops for the magnetic field minimization. *International Journal of Applied Electromagnetics and Mechanics*, Feb. 2018, vol. 56, pp. 97-106. doi: https://doi.org/10.3233/jae-172286.

19. Canova A., Giaccone L., Cirimele V. Active and passive shield for aerial power lines. *Proc. of the 25th International Conference on Electricity Distribution (CIRED 2019)*, paper no. 1096.

20. Houicher S.-E., Djekidel R., Bessidek S.A. Optimized passive and active shielding of magnetic induction generated by ultra-high-voltage overhead power lines. *International Journal of Electrical and Computer Engineering (IJECE)*, 2025, vol. 15, no. 6, pp. 5144-5161. doi: https://doi.org/10.11591/ijece.v15i6.pp5144-5161.

21. Meng Q., Wang Z., Lin Q., Ju D., Liang X., Xian D. Theoretical Analysis of a Magnetic Shielding System Combining Active and Passive Modes. *Nanomaterials*, 2024, vol. 14, no. 6, art. no. 538. doi: https://doi.org/10.3390/nano14060538.

22. Cruz P., Izquierdo C., Burgos M., Ferrer L.F., Soto F., Llanos C., Pacheco J.D. Magnetic field mitigation in power lines with passive and active loops. *CIGRE Session Materials*, 2002, reference 36-107.

23. Radwan R.M., Abdel-Salam M., Samy M.M., Mahdy A.M. Passive and active shielding of magnetic fields underneath overhead transmission lines theory versus experiment. *17th International Middle East Power Systems Conference*, 2015. pp. 1-10.
24. Radwan R., Abdel-Salam M., Mahdy A., Samy M. Laboratory Validation of Calculations of Magnetic Field Mitigation Underneath Transmission Lines Using Passive and Active Shield Wires. *Innovative Systems Design and Engineering*, 2011, vol. 2, no. 4, pp. 218-232.
25. Ziolkowski M., Gratkowski S. Active, passive and dynamic shielding of static and low frequency magnetic fields. *15th International Symposium on Theoretical Engineering*, 2009, pp. 370-374.
26. Grinchenko V.S. Mitigation of three-phase power line magnetic field by grid electromagnetic shield. *Technical Electrodynamics*, 2018, no. 4, pp. 29-32. (Ukr). doi: https://doi.org/10.15407/techned2018.04.029.
27. Celozzi S. Active compensation and partial shields for the power-frequency magnetic field reduction. *2002 IEEE International Symposium on Electromagnetic Compatibility*, Minneapolis, MN, USA, 2002, vol. 1, pp. 222-226. doi: https://doi.org/10.1109/isemc.2002.1032478.
28. Celozzi S., Garzia F. Active shielding for power-frequency magnetic field reduction using genetic algorithms optimization. *IEE Proceedings - Science, Measurement and Technology*, 2004, vol. 151, no. 1, pp. 2-7. doi: https://doi.org/10.1049/ip-smt:20040002.
29. Celozzi S., Garzia F. Magnetic field reduction by means of active shielding techniques. *WIT Transactions on Biomedicine and Health*, 2003, vol. 7, pp. 79-89. doi: https://doi.org/10.2495/ehr030091.
30. Martynenko G. Analytical Method of the Analysis of Electromagnetic Circuits of Active Magnetic Bearings for Searching Energy and Forces Taking into Account Control Law. *2020 IEEE KhPI Week on Advanced Technology (KhPIWeek)*, 2020, pp. 86-91. doi: https://doi.org/10.1109/KhPIWeek51551.2020.9250138.
31. Popov A., Tserne E., Volosyuk V., Zhyla S., Pavlikov V., Ruzhentsev N., Dergachov K., Havrylenko O., Shmatko O., Averyanova Y., Ostroumov I., Kuzmenko N., Sushchenko O., Zaliskyi M., Solomentsev O., Kuznetsov B., Nikitina T. Invariant Polarization Signatures for Recognition of Hydrometeors by Airborne Weather Radars. *Computational Science and Its Applications – ICCSA 2023. Lecture Notes in Computer Science*, 2023, vol. 13956, pp. 201-217. doi: https://doi.org/10.1007/978-3-031-36805-9_14.
32. Sushchenko O., Averyanova Y., Ostroumov I., Kuzmenko N., Zaliskyi M., Solomentsev O., Kuznetsov B., Nikitina T., Havrylenko O., Popov A., Volosyuk V., Shmatko O., Ruzhentsev N., Zhyla S., Pavlikov V., Dergachov K., Tserne E. Algorithms for Design of Robust Stabilization Systems. *Computational Science and Its Applications – ICCSA 2022. ICCSA 2022. Lecture Notes in Computer Science*, 2022, vol. 13375, pp. 198-213. doi: https://doi.org/10.1007/978-3-031-10522-7_15.
33. Ostroverkhov M., Chumack V., Monakhov E., Ponomarev A. Hybrid Excited Synchronous Generator for Microhydropower Unit. *2019 IEEE 6th International Conference on Energy Smart Systems (ESS)*, Kyiv, Ukraine, 2019, pp. 219-222. doi: https://doi.org/10.1109/ess.2019.8764202.
34. Ostroverkhov M., Chumack V., Monakhov E. Ouput Voltage Stabilization Process Simulation in Generator with Hybrid Excitation at Variable Drive Speed. *2019 IEEE 2nd Ukraine Conference on Electrical and Computer Engineering (UKRCON)*, Lviv, Ukraine, 2019, pp. 310-313. doi: https://doi.org/10.1109/ukrcon.2019.8879781.
35. Tytiuk V., Chornyi O., Baranovskaya M., Serhiienko S., Zachepa I., Tsvirkun L., Kuznetsov V., Tryputen N. Synthesis of a fractional-order $PI^{\lambda}D^{\mu}$-controller for a closed system of switched reluctance motor control. *Eastern-European Journal of Enterprise Technologies*, 2019, no. 2 (98), pp. 35-42. doi: https://doi.org/10.15587/1729-4061.2019.160946.
36. Shchur I., Turkovskyi V. Comparative Study of Brushless DC Motor Drives with Different Configurations of Modular Multilevel Cascaded Converters. *2020 IEEE 15th International Conference on Advanced Trends in Radioelectronics, Telecommunications and Computer Engineering (TCSET)*, Lviv-Slavske, Ukraine, 2020, pp. 447-451. doi: https://doi.org/10.1109/tcset49122.2020.235473.
37. Volosyuk V., Zhyla S., Pavlikov V., Ruzhentsev N., Tserne E., Popov A., Shmatko O., Dergachov K., Havrylenko O., Ostroumov I., Kuzmenko N., Sushchenko O., Averyanova Yu., Zaliskyi M., Solomentsev O., Kuznetsov B., Nikitina T. Optimal Method for Polarization Selection of Stationary Objects Against the Background of the Earth's Surface. *International Journal of Electronics and Telecommunications*, 2022, vol. 68, no. 1, pp. 83-89. doi: https://doi.org/10.24425/ijet.2022.139852.
38. Halchenko V., Trembovetska R., Bazilo C., Tychkova N. Computer Simulation of the Process of Profiles Measuring of Objects Electrophysical Parameters by Surface Eddy Current Probes. *Lecture Notes on Data Engineering and Communications Technologies*, 2023, vol. 178, pp. 411-424. doi: https://doi.org/10.1007/978-3-031-35467-0_25.
39. Halchenko V., Bacherikov D., Filimonov S., Filimonova N. Improvement of a Linear Screw Piezo Motor Design for Use in Accurate Liquid Dosing Assembly. *Smart Technologies in Urban Engineering. STUE 2022. Lecture Notes in Networks and Systems*, 2023, vol. 536, pp. 237-247. doi: https://doi.org/10.1007/978-3-031-20141-7_22.
40. Maksymenko-Sheiko K.V., Sheiko T.I., Lisin D.O., Petrenko N.D. Mathematical and Computer Modeling of the Forms of Multi-Zone Fuel Elements with Plates. *Journal of Mechanical Engineering*, 2022, vol. 25, no. 4, pp. 32-38. doi: https://doi.org/10.15407/pmach2022.04.032.
41. Hontarovskyi P.P., Smetankina N.V., Ugrimov S.V., Garmash N.H., Melezhyk I.I. Computational Studies of the Thermal Stress State of Multilayer Glazing with Electric Heating. *Journal of Mechanical Engineering*, 2022, vol. 25, no. 1, pp. 14-21. doi: https://doi.org/10.15407/pmach2022.02.014.
42. Kostikov A.O., Zevin L.I., Krol H.H., Vorontsova A.L. The Optimal Correcting the Power Value of a Nuclear Power Plant Power Unit Reactor in the Event of Equipment Failures. *Journal of Mechanical Engineering*, 2022, vol. 25, no. 3, pp. 40-45. doi: https://doi.org/10.15407/pmach2022.03.040.
43. Rusanov A.V., Subotin V.H., Khoryev O.M., Bykov Y.A., Korotaiev P.O., Ahibalov Y.S. Effect of 3D Shape of Pump-Turbine Runner Blade on Flow Characteristics in Turbine Mode. *Journal of Mechanical Engineering*, 2022, vol. 25, no. 4, pp. 6-14. doi: https://doi.org/10.15407/pmach2022.04.006.
44. Kurennov S., Smetankina N., Pavlikov V., Dvoretskaya D., Radchenko V. Mathematical Model of the Stress State of the Antenna Radome Joint with the Load-Bearing Edging of the Skin Cutout. *Lecture Notes in Networks and Systems*, 2022, vol. 305, pp. 287-295. doi: https://doi.org/10.1007/978-3-030-83368-8_28.
45. Kurennov S., Smetankina N. Stress-Strain State of a Double Lap Joint of Circular Form. Axisymmetric Model. *Lecture Notes in Networks and Systems*, 2022, vol 367 LNNS, pp. 36-46. doi: https://doi.org/10.1007/978-3-030-94259-5_4.
46. Smetankina N., Merkulova A., Merkulov D., Misiura S., Misiura I. Modelling Thermal Stresses in Laminated Aircraft Elements of a Complex Form with Account of Heat Sources. *Lecture Notes in Networks and Systems*, 2023, vol. 534 LNNS, pp. 233-246. doi: https://doi.org/10.1007/978-3-031-15944-2_22.
47. Hashim F.A., Hussain K., Houssein E.H., Mabrouk M.S., Al-Atabany W. Archimedes optimization algorithm: a new metaheuristic algorithm for solving optimization problems. *Applied Intelligence*, 2021, vol. 51, no. 3, pp. 1531-1551. doi: https://doi.org/10.1007/s10489-020-01893-z.
48. Baranov M.I., Rozov V.Y., Sokol Y.I. To the 100th anniversary of the National Academy of Sciences of Ukraine – the cradle of domestic science and technology. *Electrical Engineering & Electromechanics*, 2018, no. 5, pp. 3-11. doi: https://doi.org/10.20998/2074-272X.2018.5.01.

Received 13.09.2025
Accepted 29.11.2025
Published 02.03.2026

B.I. Kuznetsov[1], *Doctor of Technical Science, Professor,*
A.S. Kutsenko[2], *Doctor of Technical Science, Professor*
T.B. Nikitina[3], *Doctor of Technical Science, Professor,*
I.V. Bovdui[1], *PhD, Senior Research Scientist,*
K.V. Chunikhin[1], *PhD, Senior Research Scientist,*
V.V. Kolomiets[3], *PhD, Assistant Professor,*
[1] Anatolii Pidhornyi Institute of Power Machines and Systems of the National Academy of Sciences of Ukraine,
2/10, Komunalnykiv Str., Kharkiv, 61046, Ukraine,
e-mail: kuznetsov.boris.i@gmail.com (Corresponding Author)
[2] National Technical University «Kharkiv Polytechnic Institute»,
2, Kyrpychova Str., Kharkiv, 61002, Ukraine.
[3] Bakhmut Education Research and Professional Pedagogical Institute V.N. Karazin Kharkiv National University,
9a, Nosakov Str., Bakhmut, Donetsk Region, 84511, Ukraine.

How to cite this article:
Kuznetsov B.I., Kutsenko A.S., Nikitina T.B., Bovdui I.V., Chunikhin K.V., Kolomiets V.V. The methodology of multi objective design of active-passive shielding system for overhead power lines magnetic field in residential buildings space based on metaheuristic optimization method. *Electrical Engineering & Electromechanics*, 2026, no. 2, pp. 40-50. doi: https://doi.org/10.20998/2074-272X.2026.2.06